Pergamon

Chemical Engineering Science, Vol. 52, No. 24, pp. 4659–4679, 1997

PII: S0009-2509(97)00307-2
0009-2509/97 $17.00 + 0.00

On the solution of population balance equations by discretization—III. Nucleation, growth and aggregation of particles*

Sanjeev Kumar† and D. Ramkrishna‡
School of Chemical Engineering, Purdue University, West Lafayette, IN 47907, USA

Abstract—A new discretization method for solving population balance equations for simultaneous nucleation, growth and aggregation of particles is proposed. The method combines the best features of our discretization technique (Kumar and Ramkrishna, 1996, *Chem. Engng. Sci.* **51**, 1311–1337), i.e., designing discrete equations to obtain desired properties of a size distribution directly, applicability to an arbitrary grid to control resolution and computational efficiency, with the method of characteristics to offer a technique which is very general, powerful and overcomes the crucial problems of numerical diffusion and stability that beset the previous techniques in this area. The proposed technique has been tested for pure growth, simultaneous growth and aggregation, and simultaneous nucleation and growth for a large number of combinations obtained by changing functions for nucleation rate, growth rate, aggregation kernel and initial condition. In all cases, the size distributions obtained from the proposed technique and those obtained analytically are in excellent agreement. The presence of moving discontinuities, which is unavoidable due to the hyperbolic nature of the governing equation, is addressed with no additional difficulty in all of the test problems. © 1997 Elsevier Science Ltd

Keywords: Population balance; discretization; nucleation; growth; aggregation; particles

1. INTRODUCTION

This paper enlists in an endeavor to felicitate Professor Manmohan Sharma on his 60th birthday for his outstanding contributions to the chemical engineering profession. Indeed, this contribution is more in tune with the abstract paradigm that deliberates on reactions of species incognito than with the vibrant creatures of live chemical technology which were the hallmark of Sharma's approach to chemical engineering. However, a major aspect of Sharma's work has been connected with dispersed phase contacting in which population balance has emerged as a crucial analytical tool. Insofar as this paper purports to deal with efficient solutions to population balance equations of dispersed systems, its target is a subject that has remained one of his fundamental interests.

Simultaneity of nucleation, growth and aggregation of particles is key to characterizing processes such as precipitation, crystallization and aerosol formation and so on. Rigorous modeling of such processes requires the framework of population balances and which leads to an an integro-partial-differential equation, also known as the population balance equation (PBE). Often, the resulting equation cannot be solved analytically and therefore numerical solutions are needed. Model-based control strategies furthermore require that the numerical solutions should be obtainable in time-scale commensurate with the process time scale.

Among the various numerical techniques proposed in the past for solving PBEs (see Ramkrishna, 1985 for a review), a recent discretization method, which considers particles of different sizes to exist in groups and interact collectively with particles in other groups (Batterham *et al.*, 1981; Hounslow *et al.*, 1988; Kostoglou and Karabelas, 1994), has emerged as an accurate and a computationally efficient alternative. In this method, the continuous size range is divided into discrete but contiguous size ranges (also called bins) using a grid, and macroscopic balance equations, conceptually similar to the well-known macroscopic balances in transport processes, are then written for the populations of bins. The above procedure converts the integro-partial-differential equation into a system of first-order ordinary differential equations

* The results contained in this paper were first presented in the 1995 annual meeting of AICHE at Miami, USA.

† Present address: Department of Chemical Engineering, Indian Institute of Science, Bangalore 560 012, India.

‡ Corresponding author.

which can be solved easily using the standard ODE integrators.

Kumar and Ramkrishna (1996, Part I) have recently proposed a new discretization technique for solving population balance equations for breakage and aggregation of particles. Here, the population of a bin is represented through a representative volume called a *pivot*. The distinct features of this technique are (i) formulation of discrete equations to obtain directly the desired properties of the size distribution instead of very accurate estimates of number density which can be computation intensive, (ii) flexibility to work with an arbitrary grid which allows a grid to be optimized with respect to resolution and accuracy; and (iii) computational efficiency. The crux of the technique is derived from the concept of *internal consistency* which requires the set of discrete equations to yield correct expressions for at least the desired properties (of which moments are special cases). Internal consistency with respect to the chosen properties is assured by ensuring that the same chosen properties of the new particles (formed due to breakage or aggregation) are exactly preserved. The technique has been demonstrated for pure breakage and pure aggregation, simultaneous breakage and aggregation, solution of discrete-continuous PBEs and prediction of second moment directly using a relatively coarse grid. For more details, the reader is referred to Part I.

Efforts have been made in the past to include particle *growth* and *nucleation* in the discrete version of PBEs. It may appear that the inclusion of growth and nucleation, which are much simpler processes than the breakage and aggregation, should be a trivial matter. However, a close look at the general equation, given below, will show that it is not quite so.

$$\frac{\partial n(v,t)}{\partial t} + \frac{\partial [G(v)n(v,t)]}{\partial v} = \frac{1}{2}\int_0^{\infty} n(v-v',t)\,n(v',t)\,q(v-v',v')\,\mathrm{d}v' - n(v,t)\int_0^{\infty} n(v',t)\,q(v,v')\,\mathrm{d}v' + S(v). \tag{1}$$

Here, $n(v,t)\,\mathrm{d}v$ is number of particles in size range v to $v + \mathrm{d}v$ at time t, $G(v)$ is growth rate for particles of size v, $S(v)$ is rate at which particles of size v are nucleated and $q(v,v')$ is aggregation frequency. Equation (1) is a hyperbolic partial differential equation because of the second (convective) term on the l.h.s. Such equations are well known for causing enormous difficulties with their numerical solution. Stability and dispersion of numerical solutions obtained using various finite difference approximations are well documented (Lapidus and Pinder, 1982).

Hounslow *et al.* (1988), Marchal *et al.* (1988) and David *et al.* (1991) have proposed straightforward extensions of discretization methods (similar to finite difference type formulae) to include growth and nucleation processes. The numerical results obtained using these techniques are shown in the next section to be unsatisfactory.

The objective of this paper is to present a new technique for solving PBEs for nucleation, growth and aggregation, all processes occurring simultaneously. The technique makes use of the best features of the discretization technique proposed in Part I in combination with the method of characteristics. The new technique is free from problems due to stability and dispersion of the numerical solution that beset earlier extensions of discretization methods.

The remaining paper is organized as follows. The next section reviews the previous work with focus on growth and nucleation terms. Section 3 contains the derivation of discrete equations. Special cases and a peculiar problem that arises with nucleation term are dealt in various subsections. Section 4 provides detailed comparisons of the numerical and analytical results for various combinations of the three processes. Conclusions are provided in Section 5.

2. PREVIOUS WORK

Kostoglou and Karabelas (1994) and Kumar and Ramkrishna (1996) have provided critical reviews of the previous work on the solution of PBEs for aggregation. This section, therefore, focuses only on nucleation and growth processes.

Middleton and Brock (1976) and Gelbard and Seinfeld (1978) have solved eq. (1) using cubic splines. Although, cubic splines facilitate easy evaluation of integral and derivative terms appearing in the equations, the technique is computationally inefficient because spline coefficients need to be evaluated at each time step. Moreover, the ability of cubic splines to handle sharp fronts, which arise due to growth and aggregation processes, has not been demonstrated.

Recently, discretization techniques for solving PBEs have emerged as powerful and computationally efficient alternatives. In this approach, the continuous size range is partitioned into various size ranges. If N_i is defined as the population of the ith size range, i.e.

$$N_i(t) = \int_{v_i}^{v_{i+1}} n(v,t)\,\mathrm{d}v, \tag{2}$$

the rate of change of N_i [explicit mention of time dependence in $N_i(t)$ is suppressed in favor of a simpler notation] due to aggregation is in general expressed as

$$\left.\frac{\mathrm{d}N_i}{\mathrm{d}t}\right|_{\text{aggregation}} = \sum_{j=1}^{i}\sum_{k=1}^{j} \alpha_{i,j,k} N_j N_k - N_i \sum_{j=1}^{M} \beta_{i,j} N_j. \tag{3}$$

The various techniques available in the literature differ from one another in how the time-invariant coefficients $\alpha_{i,j,k}$'s and $\beta_{i,j}$'s are evaluated.

An expression for $\mathrm{d}N_i/\mathrm{d}t$ due to only nucleation and growth processes, obtained by integrating eq. (1)

from v_i to v_{i+1} for $q(v,v') = 0$, is given as

$$\left.\frac{dN_i}{dt}\right|_{\text{nucleation \& growth}} = G(v_i)n(v_i,t) - G(v_{i+1})n(v_{i+1},t) + \int_{v_i}^{v_{i+1}} S(v)\,dv. \quad (4)$$

2.1. *Representation of nucleation*

Equation (4) shows that the inclusion of nucleation in discrete equations is quite straightforward. The most common choice for $S(v)$ in $\dot{N}_{0,n}\delta(v - v_0)$, where v_0 belongs to the first bin (Hounslow *et al.*, 1988; Marchal *et al.*, 1988; David *et al.*, 1991). The nucleation term therefore appears only in the equation for the population of the first bin. Thus,

$$\left.\frac{dN_i}{dt}\right|_{\text{nucleation}} N_{0,n}\delta_{i,1}. \quad (5)$$

The set of equations in eq. (4) needs estimates of number density at bin boundaries to provide a closed system of equations.

2.2. *Representaton of growth*

Marchal *et al.* (1988) have followed the simple strategy of replacing the number density at a boundary by the arithmetic mean of the average number densities on either side of it. Thus,*

$$n(v_i,t) = \frac{1}{2}\left(\frac{N_{i-1}}{\Delta v_{i-1}} + \frac{N_i}{\Delta v_i}\right). \quad (6)$$

In a later paper, the authors (David *et al.*, 1991) have chosen a different expression for estimating $n(v_i,t)$:

$$n(v_i,t) = \frac{\Delta v_{i-1}\,N_i/\Delta v_i + \Delta v_i N_{i-1}/\Delta v_{i-1}}{\Delta v_{i-1} + \Delta v_i}. \quad (7)$$

Δv_i, the width of the ith bin is defined as $v_{i+1} - v_i$.

Hounslow *et al.* (1988) have extended their discretization technique for aggregation to size-independent particle growth [$G(v) = \sigma_0$] by choosing the following form for dN_i/dt:

$$\left.\frac{dN_i}{dt}\right|_{\text{growth}} = \frac{\sigma_0}{v_i}(aN_{i-1} + bN_i + cN_{i+1}) \quad (8)$$

and then estimating coefficients a, b and c by forcing eq. (8) to yield the correct expressions for three moments. Their final set of equations is

$$\left.\frac{dN_i}{dt}\right|_{\text{growth}} = \frac{2\sigma_0}{(1+r)v_i}\left[\left(\frac{r}{r^2-1}\right)(N_{i-1} - N_{i+1}) + N_i\right] \quad (9)$$

where $r = v_{i+1}/v_i$. Equation (9) when rearranged to fit the form of eq. (4) yields

$$\left.\frac{dN_i}{dt}\right|_{\text{growth}} = \sigma_0\left[\left(\frac{2}{1+r}\frac{N_{i-1} + rN_i}{v_{i+1} - v_{i-1}}\right) - \left(\frac{2}{1+r}\frac{N_i + rN_{i+1}}{v_{i+2} - v_i}\right)\right] \quad (10)$$

such that

$$n(v_i,t) = \frac{2}{1+r}\left(\frac{N_{i-1} + rN_i}{v_{i+1} - v_{i-1}}\right). \quad (11)$$

The discretized equations for all the three techniques discussed here have the potential to produce negative values of N_i's. However, only Hounslow *et al.* have mentioned it explicitly and indicated that meaningful results can still be obtained merely by setting negative N_i's to zero. The authors have proposed a different discretization of the growth term in the presence of nucleation:

$$\frac{dN_i}{dt} = \sigma_0\frac{N_{i-1}}{v_i - v_{i-1}} - \sigma_0\frac{N_i}{v_{i+1} - v_i} \quad (12)$$

To compare the effectiveness of these three techniques, we have solved† eq. (4) for $G(v) = 1$, and

$$n(v,0) = N_{0,i}\frac{1}{v_{0,i}}\exp(-v/v_{0,i})$$

using each technique, i.e., $n(v_i,t)$ in eq. (4) has been replaced by expressions in eqs (6), (7), and (11). The numerical and the analytical results are shown in Figs 1(a) and (b) using linear and log scales, respectively. The figures show that the results obtained by the technique of Marchal *et al.* (1988) oscillate a great deal in the region where the analytical number density is zero. The technique of David *et al.* (1991) shows damped oscillations. In the tail region, all the three techniques make similar overpredictions due to numerical diffusion [this term is used to indicate the errors that arise when the discrete or finite difference version of a partial differential equation actually corresponds to a different original equation, one with an added diffusion term! see Lapidus and Pinder (1982) for more details]. The technique of Hounslow *et al.* (1988) does not show oscillations because the negative values were set to zero, as recommended by them. All the three techniques make incorrect predictions of the location of the discontinuity. If the negative N_i are set to zero in the techniques proposed by Marchal *et al.* (1988) and David *et al.* (1991), the oscillations

*Some authors have worked with crystal length as the internal coordinate. In the presence of aggregation, particle size appears to be a better choice as it simplifies the aggregation terms. This however changes a size-independent rate of change of linear dimension to a size-dependent rate in terms of particle volume and *vice versa*.

†The cases consider here for testing the numerical techniques reviewed above are the same as those considered by Hounslow *et al.* (1988) to demonstrate their technique for pure growth and simultaneous nucleation and growth.

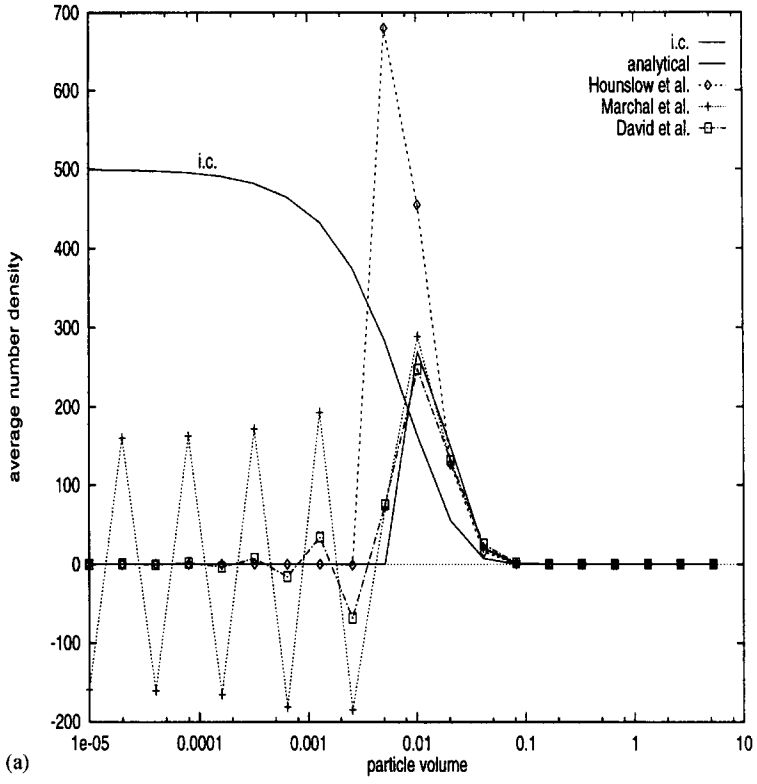

(a)

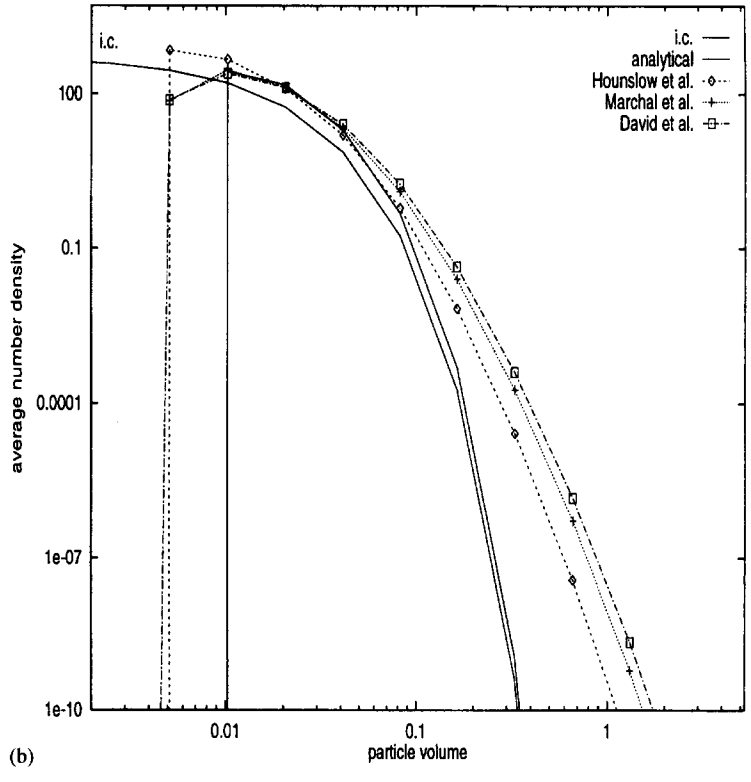

(b)

Fig. 1. A comparison of size distributions obtained using various techniques at $t = 0.01$ for pure growth $[G(v) = 1]$ of an exponentially distributed initial population (a) linear-log scale; (b) log–log scale.

disappear and the predictions become similar to those of Hounslow *et al.* (1988).

We have also tested these techniques for their ability to represent a nucleation process. A simple case of simultaneous nucleation of mono-sized nuclei, size-independent growth rate with zero initial population is considered. Simulations using the techniques of Marchal *et al.* and David *et al.* employ the same equations as in the previous case; however, the technique of Hounslow *et al.* requires a different set of equations [contained in eq. (12)]. Nucleation is represented through an additional term in equation for N_1 in all the three techniques. Figures 2(a) and 2(b) show the same numerical and the analytical results on a linear and a log scale, respectively. The figure shows that once again, the results obtained using the techniques of Marchal *et al.* and David *et al.* oscillate about the analytical solutions. The technique of Hounslow *et al.* makes good predictions in this region. The numerical solutions around the location of the discotinuity are highly diffused for all the three techniques, however. This is quite natural for finite-difference-type approximations as they have an infinite velocity of propagation for the signal.

In an effort to overcome these deficiencies, Muhr *et al.* (1995, 1996) chose to solve the finite-difference version of eq. (1) for *growth* and *nucleation* only. The authors used the well-known *methods of lines* which converts a PDE to a set of ODEs. In their first paper, the authors used a central difference for the growth term which led to negative values (pointed out in their second paper) irrespective of how fine the spatial grid was. This is hardly surprising since central difference in space and forward difference in time is known to be unconditionally unstable (Lapidus and Pinder, 1982). The authors sought to remedy this situation by choosing an upwind difference scheme in their second paper. However, use of an excessively fine spatial grid was required to reach convergence with respect to total numbers. It is not clear whether the size distributions also converged. Upwind difference approximation is known to have excessive diffusion (Lipidus and Pinder, 1982), and therefore, acceptable solutions can result only when an excessively fine grid is used. The same holds for the method of lines (Schiesser, 1991). It appears that the same factors as those responsible for the poor performance of the finite-difference approximations are also responsible for the poor performance of approximations in eqs (6), (7) and (11). A rigorous analysis is needed, however.

It is clear from this section that the existing methods for extending discretization methods to include growth processes are not adequate. In the next section, we develop a new procedure for solving PBEs representing nucleation, growth and aggregation of particles.

3. FORMULATION OF DISCRETE EQUATIONS

We start with the general population balance equation (1) which after differentiating the growth term by parts yields

$$\frac{\partial n(v,t)}{\partial t} + G(v)\frac{\partial n(v,t)}{\partial v} + n(v,t)\frac{\mathrm{d}G(v)}{\mathrm{d}v} = \frac{1}{2}\int_0^v n(v-v',t)n(v',t)q(v-v',v')\,\mathrm{d}v' - n(v,t)\int_0^\infty n(v',t)q(v,v')\,\mathrm{d}v' + S(v). \tag{13}$$

Substituting for the growth rate $G(v)$, defined as

$$\frac{\mathrm{d}v}{\mathrm{d}t} = G(v), \tag{14}$$

we obtain

$$\frac{\partial n(v,t)}{\partial t} + \frac{\partial n(v,t)}{\partial v}\frac{\mathrm{d}v}{\mathrm{d}t} + n(v,t)\frac{\mathrm{d}G(v)}{\mathrm{d}v} = \text{r.h.s. of eq. (13)}. \tag{15}$$

Defining a total derivative of the number density

$$\frac{\mathrm{d}n(v,t)}{\mathrm{d}t} = \frac{\partial n(v,t)}{\partial t} + \frac{\partial n(v,t)}{\partial v}\frac{\mathrm{d}v}{\mathrm{d}t} \tag{16}$$

and substituting it in eq. (15) leads to

$$\frac{\mathrm{d}n(v,t)}{\mathrm{d}t} + n(v,t)\frac{\mathrm{d}G(v)}{\mathrm{d}v} = \frac{1}{2}\int_0^v n(v-v',t)n(v',t)q(v-v',v')\,\mathrm{d}v' - n(v,t)\int_0^\infty n(v',t)q(v,v')\,\mathrm{d}v' + S(v). \tag{17}$$

Equation (17) describes the variation of number of density of particles of size v noticed by an observer moving in the particle volume phase space with the growth velocity of the particles being observed. Thus, eq. (17) together with eq. (14) which describes the motion of the observer completely specify the system. The mathematical procedure of transforming eq. (1) to eqs (14) and (17) and solving the latter for a solution is called the 'method of characteristics'. It is important to point out here that particle volume v in eq. (17) is not an independent variable, but rather a function of time. We will now combine the method of characteristics with the method of discretization of Part I to obtain an efficient and accurate technique for solving eq. (1).

Consider the size range of interest to be discretized into contiguous size ranges (bins) as shown in Fig. 3. Let the smallest and the largest sizes for ith size range be denoted by v_i and v_{i+1}, respectively. Since eq. (17) describes change in number density for an observer moving at particle growth velocity, we consider the grid boundaries to also move with the growth velocity

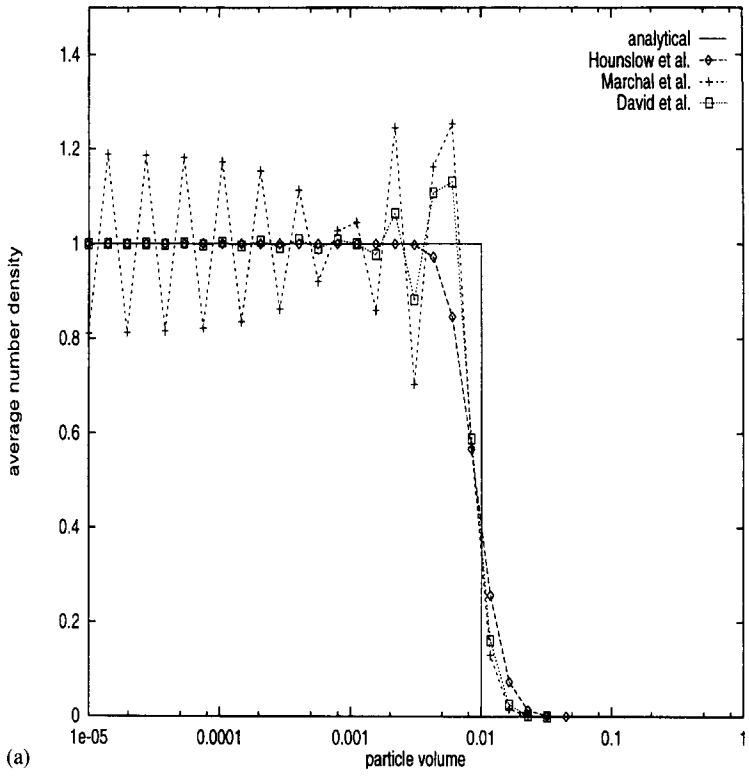

(a)

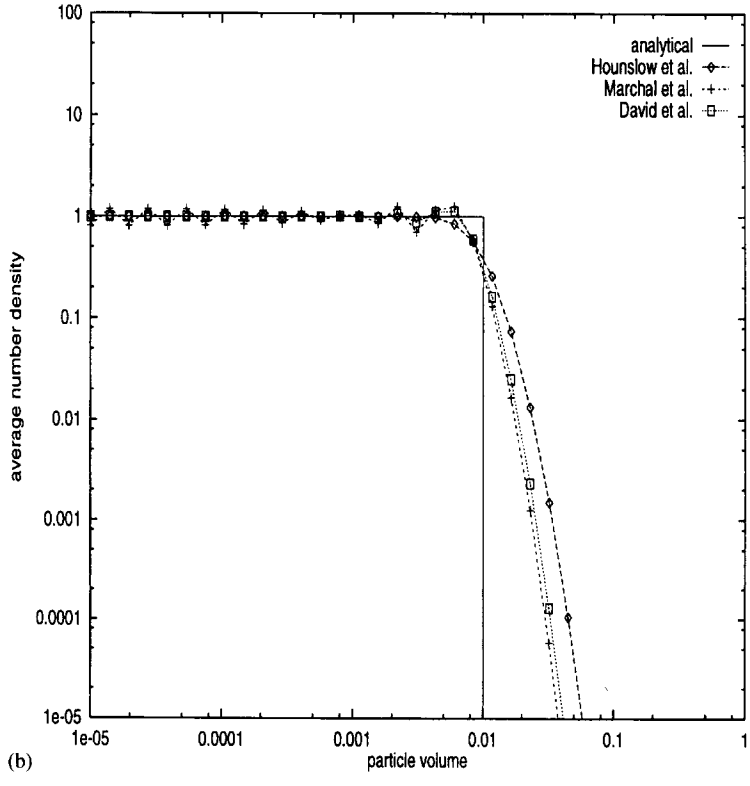

(b)

Fig. 2. A comparison of size distributions obtained using various techniques at $t = 0.01$ for pure growth $[S(v) = 1\delta(v - 1 \times 10^{-5})]$ and pure growth $[G(v) = 1]$ with zero initial population (a) linear-log scale; (b) log–log scale.

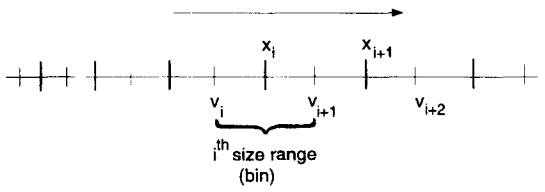

Fig. 3. A typical moving grid.

of the particles they represent, i.e.

$$\frac{dv_i}{dt} = G(v_i) \tag{18a}$$

$$\frac{dv_{i+1}}{dt} = G(v_{i+1}) \tag{18b}$$

The rate of change of total number of particles in ith size range (both size range and population contained in it can change with time) can now be obtained by integrating eq. (17) with respect to v from $v_i(t)$ to $v_{i+1}(t)$. Thus,

$$\int_{v_i(t)}^{v_{i-1}(t)} \frac{dn(v,t)}{dt} dv + \int_{v_i(t)}^{v_{i+1}(t)} n(v,t) \frac{dG(v)}{dv} dv = \int_{v_i(t)}^{v_{i-1}(t)} [\text{r.h.s. of eq. (17)}]\, dv \tag{19}$$

Integrating the second term on the l.h.s. by parts, we obtain

$$\int_{v_i(t)}^{v_{i-1}(t)} \frac{dn(v,t)}{dt} dv + |n(v,t)G(v)|_{v_i}^{v_{i+1}} - \int_{v_i(t)}^{v_{i+1}(t)} G(v) \frac{\partial n(v,t)}{\partial v} dv = \int_{v_i(t)}^{v_{i+1}(t)} [\text{r.h.s. of eq. (17)}]\, dv. \tag{20}$$

Combining the first and third terms on the l.h.s. using eq. (16) and substituting for $G(v)$, the above equation reduces to

$$\int_{v_i(t)}^{v_{i-1}(t)} \frac{\partial n(v,t)}{\partial t} dv + \left| \frac{dv}{dt} n(v,t) \right|_{v_i}^{v_{i+1}} = \int_{v_i(t)}^{v_{i+1}(t)} [\text{r.h.s. of eq. (17)}]\, dv. \tag{21}$$

Using Leibnitz formula, and substituting the r.h.s. of eq. (17), the following equation is obtained:

$$\frac{d}{dt} \int_{v_i(t)}^{v_{i-1}(t)} n(v,t)\, dv = \frac{1}{2} \int_{v_i(t)}^{v_{i+1}(t)} dv \int_0^v n(v-v',t) n(v',t) q(v-v',v)\, dv' - \int_{v_i(t)}^{v_{i-1}(t)} dv \int_0^\infty n(v,t) n(v',t) q(v,v')\, dv' + \int_{v_i(t)}^{v_{i-1}(t)} S(v)\, dv. \tag{22}$$

For a special case of $q(v,v') = 0$ and $S(v) = 0$, eq. (22) reduces to the following:

$$\frac{d}{dt} \int_{v_i(t)}^{v_{i-1}(t)} n(v,t) dv = 0. \tag{23}$$

This simple equation indicates that in the absence of nucleation and aggregation, the total number of particles in a size range, whose boundaries move as particles grow, does not change with time. The result, of course, follows from the fact that the time derivative in eq. (23) considers a fixed collection of particles. Starting from this result, which is quite intuitive for pure growth and did not require a derivation, Gelbard (1990) and Kim and Seinfeld (1990) have developed a moving sectional technique for pure growth of aerosol particles. The technique yielded good results. They, however, argued that the approach was unsuitable for extension to particle aggregation and considered it to be its major weakness. The nucleation of new particles, which we will later see to be a still more difficult issue, was ignored by these authors.

We now propose that the total population of the ith size range be represented by a representative volume x_i, and as before, call it the ith pivot. The complete number density function can therefore be written as

$$n(v,t) = \sum_{i=1}^{i=M} N_i(t) \delta(v - x_i). \tag{24}$$

The particle volume v in eq. (22) changes with time and since x_i is like any other particle size, it also changes with time:

$$\frac{dx_i}{dt} = G(x_i). \tag{25}$$

When particles are considered to exist only at pivots, aggregation of smaller particles can lead to formation of particles of sizes different from the chosen pivots. In Part I, we have proposed that such particles should be represented through the adjoining pivots in a way that preserves the desired properties of the original particle. Using this simple concept, it is claimed there that the resulting discrete equations become *internally consistent* with respect to at least the chosen properties– the equations, when manipulated, give correct expressions for the chosen properties for the whole size distribution. Thus, if one of the preserved properties is $f_i(v)$, the discrete equations for $N_j(t)$, when multiplied by $f_i(x_j)$ and added over all bins, provide correct expression for

$$\frac{d}{dt} \int_0^x f_i(v) n(v,t)\, dv.$$

In principle, one can preserve any even number of properties, say 2ν of them, by assigning a newly formed particle to ν pivots of volumes smaller than the volume of the newly formed particle and another ν pivots of larger volumes.

Using these concepts, the aggregation terms on the r.h.s. of eq. (22) for zero growth, which are given as

$$\frac{1}{2}\int_{v_i}^{v_{i+1}} dv \int_0^v n(v-v',t)n(v',t)q(v-v',v')\,dv' - \int_{v_i}^{v_{i+1}} n(v,t)\,dv \int_0^\infty n(v',t)q(v,v')\,dv' \quad (26)$$

were discretized by us in Part I to obtain

$$\sum_{x_{i-1}\leqslant(x_j+x_k)\leqslant x_{i+1}}^{i\geqslant j\geqslant k} (1-\tfrac{1}{2}\delta_{j,k})\eta q_{j,k}N_j(t)N_k(t) - N_i(t)\sum_{k=1}^{M} q_{i,k}N_k(t) \quad (27)$$

where η for the preservation of two power-law-type properties, v^ζ and v^ν, is given by

$$\eta = \begin{cases} \dfrac{v^\zeta x_{i+1}^\nu - v^\nu x_{i+1}^\zeta}{x_i^\zeta x_{i+1}^\nu - x_i^\nu x_{i+1}^\zeta}, & x_i \leqslant v \leqslant x_{i+1} \\ \dfrac{v^\zeta x_{i-1}^\nu - v^\nu x_{i-1}^\zeta}{x_i^\zeta x_{i-1}^\nu - x_i^\nu x_{i-1}^\zeta}, & x_{i-1} \leqslant v \leqslant x_i \end{cases} \qquad v = x_j + x_k \quad (28)$$

and $q_{i,j}$ is $q(x_i, x_j)$.

The aggregation terms on the r.h.s. of eq. (22) differ from the terms in eq. (26) only in that v_i's and x_i's for the former are time-dependent quantities while they are constant for the latter. Since, these terms consist of only integrations with respect to volume, the discrete approximation for the case of time-invariant v_i's and x_i's can be used for time-dependent v_i's and x_i's as well provided the v_i's and x_i's in eqs (27) and (28) are treated as time-dependent.

Thus, substituting for $n(v,t)$ from eq. (24) and making use of the approximation developed in Part I, the following set of final equations is obtained:

$$\frac{dN_i(t)}{dt} = \sum_{\substack{j,k \\ x_{i-1}(t)\leqslant(x_j(t)+x_k(t))\leqslant x_{i+1}(t)}}^{i\geqslant j\geqslant k} (1-\tfrac{1}{2}\delta_{j,k})\eta q_{j,k}N_j(t)N_k(t) - N_i(t)\sum_{k=1}^{M} q_{i,k}N_k(t) + \int_{v_i(t)}^{v_{i+1}(t)} S(v)\,dv \quad (29a)$$

and

$$\frac{dx_i}{dt} = G(x_i). \quad (29b)$$

The coefficients $q_{i,j}$ in eq. (29a) are evaluated as $q(x_i(t), x_j(t))$ and η, for the preservation of two properties v^ζ and v^ν, is given as

$$\eta = \begin{cases} \dfrac{v^\zeta x_{i+1}^\nu(t) - v^\nu x_{i+1}^\zeta(t)}{x_i^\zeta(t)x_{i+1}^\nu(t) - x_i^\nu(t)x_{i+1}^\zeta(t)}, & x_i(t) \leqslant v \leqslant x_{i+1}(t) \\ \dfrac{v^\zeta x_{i-1}^\nu(t) - v^\nu x_{i-1}^\zeta(t)}{x_i^\zeta(t)x_{i-1}^\nu(t) - x_i^\nu(t)x_{i-1}^\zeta(t)}, & x_{i-1}(t) \leqslant v \leqslant x_i(t) \end{cases}$$
$$v = x_j(t) + x_k(t). \quad (30)$$

The above expression for η simplifies to the following for the preservation of number and mass:

$$\eta = \begin{cases} \dfrac{x_{i+1}(t) - v}{x_{i+1}(t) - x_i(t)}, & x_i(t) \leqslant v \leqslant x_{i+1}(t) \\ \dfrac{x_{i-1}(t) - v}{x_{i-1}(t) - x_i(t)}, & x_{i-1}(t) \leqslant v \leqslant x_i(t) \end{cases}$$
$$v = x_j(t) + x_k(t). \quad (31)$$

The set of equations in eq. (29) with accompanying definitions in eqs (30) or (31) represents the final system of equations for solving a general problem involving simultaneous nucleation, growth and aggregation. For specific cases of interest, the above system of equations either reduces to simpler equations or requires special considerations for its implementation. These specific cases are now discussed in the following subsections.

3.1. *Pure growth*

For the situation of pure growth $q(v,v') = S(v) = 0$, the simplified system of equations is given by

$$\frac{dx_i}{dt} = G(x_i). \quad (32)$$

The set of equations for N_i's drop out because N_i's do not change with time for $q(v,v') = S(v) = 0$. The time-dependent v_i's can be obtained from $x_i(t)$'s using the definition $v_i = (x_{i-1} + x_i)/2$ for simple growth functions $G(v) = \sigma_0$ or $\sigma_0 v$. Otherwise, differential equations identical to those for x_i's can be set up and solved for to obtain time-dependent v_i's as well.

3.2. *Simultaneous growth and aggregation*

Simultaneous growth and aggregation of particles is characterized by eq. (29) with $S(v) = 0$. The numerical solutions can be obtained by solving these equations in their present form, but it requires the inequalities in eq. (29a) to be evaluated at every time step. This, however, is not necessary. The possible aggregation events that contribute to the population at a given pivot change only slowly. In fact, for $G(v) = kv$, they do not change at all! The results of the inequality tests can therefore be stored in some usable form and need to be updated only at some regular intervals. In this paper, we have chosen the latter strategy. It is however conceivable that the inequalities be updated automatically when x_i's have changed by more than some acceptable level.

Aggregation of particles results in formation of increasingly larger size of particles and is conventionally handled by starting with a size range large enough to accommodate all particle sizes that come to exist at the desired final time. The distribution at the final time, however, becomes known only after the equations are solved and therefore this procedure involves some amount of trial-and-error, experience and a safety margin. Furthermore, it entails uncessary computations as the bins for large size particles

acquire meaningful populations only towards the end of the simulation and need not be present all through. In spite of these shortcomings, we have followed the same approach as the focus of the paper is on discretization of growth and nucleation terms. More efficient strategies that overcome these deficiencies have been implemented, however, and will be discussed separately along with other relevant issues.

3.3. *Presence of nucleation*

The method of characteristics combined with the discretization concepts obviates the discretization of the growth term to overcome the problems of diffusion and stability that impaired the earlier techniques. Unfortunately, nucleation of particles which was incorporated quite easily in earlier techniques now poses a new difficulty. Nucleating particles have to appear as new population in one of the bins and since the bins move with time, a situation arises when some or all of the nuclei become smaller than the smallest particle size represented in the bins, and the nucleation term cannot be represented accurately. This is also evident from eq. (29a) for $i = 1$.

A simple solution to this problem lies in adding new bins, one at a time, with zero population at the small size end at regular intervals. To illustrate it clearly, we consider a general example of simultaneous nucleation of mono-dispersed nuclei, growth of particles and their aggregation. The size of the nuclei and the generation rate are allowed to be time dependent. Thus,

$$S(v,t) = \dot{N}_{0,n}(t)\delta(v - v_{0,n}(t)). \tag{33}$$

The rate of change of nuclei size, $dv_0(t)/dt$, is taken to be smaller than $G(v_0)$ so that the size of the nuclei becomes smaller than the smallest size represented by the first bin at some finite time. In this example, we, however, consider $dv_0(t)/dt = 0$. Let us now assume that at initial time, the nuclei are born into the second bin, as shown in Fig. 4(a). As time progresses, the bins move to larger sizes while the size of the nuclei does not and eventually the nuclei start feeding the first bin. After a short while, $v_1(t)$, the lower boundary of the first bin coincides with the nuclei size, and from now on, the nuclei cannot be fed to any of the original bins. We now add a new bin with the following characteristics: $v_1 = v_2 = x_1 = v_{0,n}$, $N_1 = 0$ and renumber the old bins as increasing sequence of integers [Fig. 4(b)]. While the movement of all the bin boundaries and pivots is given by the equations obtained before, the movement of v_1 and x_1 is handled differently. The lower boundary of the first bin, v_1, stays with $v_0(t)$, the size of the nuclei, and x_1, the representative volume for the first bin, stays in the middle of the bin:

$$\frac{dv_1}{dt} = \frac{dv_0(t)}{dt} \tag{34a}$$

$$\frac{dx_1}{dt} = \frac{1}{2}\left(\frac{dv_1}{dt} + \frac{dv_2}{dt}\right). \tag{34b}$$

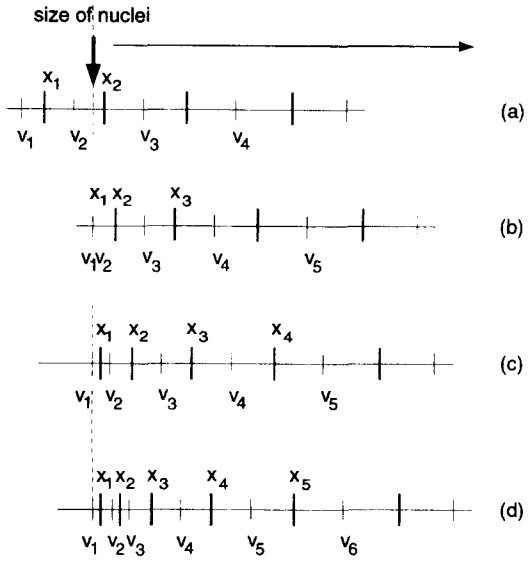

Fig. 4. An illustration of how nucleation of particles is incorporated into a moving grid.

The equation for N_1 is the same as that for any other N_i. The above representation correctly accounts for both the mass and the number of the nuclei for constant and linear growth rates and for linear or no changes in $v_0(t)$ with time. For more complex rate laws, the number of nuclei, which determine the number of large size particles appearing later, are guaranteed to be accounted correctly. The mass of nuclei, which is only an insignificant fraction of the total mass, may not be represented correctly. It is however not difficult to arrive at more complex procedures that will preserve the desired properties of the nuclei. It is important to point out here that the particles nucleating in the first bin also are lost due to their aggregation with particles in all bins including the first one. So, if there are any interesting features that are present in the size range close to the nuclei size, they will be reflected accurately in the numerical results.

The set of equations which includes the equations for the new bin is solved for only a small time Δt which is chosen to be the time required for the newly added bin to grow from zero width to a new width that is commensurate with the desired resolution in this size range [Fig. 4(c)]. If the first bin is allowed to grow to become too wide, the aggregation of particles within the same bin will not be accounted correctly. After time Δt, a new bin like the one before is added, bins are renumbered and the process continues on.

Using this simple strategy, it is possible to address many complex situations, i.e. dissolution of some particles while the others grow or initially all particles grow but at a later time, small ones start dissolving. The inclusion of these complexities requires only a moderate effort. In this paper, therefore, we will concentrate only on elucidating the basic technique.

One obvious difficulty with the above procedure is that the width of the newly added bins, much after

they were first added, depends on the rate law for particle growth. For linear growth rate law,

$$\frac{dv}{dt} = \sigma_0 v$$

the width of the newly added bins keeps on increasing because the boundaries of the bins grow at differential rates. This is a desirable feature as it automatically gives rise to a geometrical grid (ratio v_{i+1}/v_i being $e^{\sigma_0 \Delta t}$). In contrast, for constant growth law, the width of newly added bins, as they move, does not change because both the boundaries of a bin move at the same rate. Thus, the addition of new bins results in a linear grid in the small size range as shown in Figs 4(c) and (d) and when new bins have moved to larger sizes, constant bin width results in a very fine grid. Clearly, the number of equations that need to be solved increases very rapidly and the technique becomes computation-intensive. The biggest advantage of discretization methods—their ability to produce size distribution with only a small number of equations—is therefore lost.

The technique of Part I once again allows us to restore the effectiveness of discretization methods by converting a fine grid into a coarse grid as the bins move to larger sizes. The objective here is to keep the relative resolution of the grid point approximately the same over most of the size range. This is accomplished by using the principles already used in assigning newly formed aggregates to the adjoining pivots. In the present situation, some of the pivots that need to be eliminated to make the grid coarse are assigned to the adjoining pivots in a way that the desired properties of the population at the pivot in question are preserved. These properties are the same as those preserved in the aggregation process. Thus, if the population at ith pivot is to be assigned to $(i-1)$th and $(i+1)$th, fractions η_{i+1} and n_{i-1} assigned to $(i+1)$th and $(i-1)$th pivots, respectively, for the preservation of v^ζ and v^ν properties are given as

$$\eta_{i+1} = \frac{x_i^\zeta x_{i-1}^\nu - x_{i-1}^\nu x_{i-1}^\zeta}{x_{i+1}^\zeta x_{i-1}^\nu - x_{i+1}^\nu x_{i-1}^\zeta}, \tag{35a}$$

$$\eta_{i-1} = \frac{x_i^\zeta x_{i+1}^\nu - x_{i-1}^\nu x_{i+1}^\zeta}{x_{i+1}^\nu x_{i-1}^\zeta - x_{i+1}^\zeta x_{i-1}^\nu}. \tag{35b}$$

4. NUMERICAL RESULTS

The technique developed in this paper can be used to simulate various combinations of nucleation, growth and aggregation for different choices of nucleation rate function, growth rate function, aggregation kernel and initial conditions. However, to inspire one's faith in the technique, it needs to be tested for the cases which can be solved analytically. The following is the list of relevant combinations of processes for which the continuous PBE has been solved analytically

(i) Pure growth.
(ii) Simultaneous growth and aggregation.
(iii) Simultaneous nucleation and growth.

PBEs for pure aggregation and simultaneous nucleation and aggregation have also been solved analytically but since these cases require the technique developed in Part I only, they have been excluded from the present investigation. Unfortunately, the technique cannot be tested for the most relevant case of simultaneous nucleation, growth and aggregation because analytical solutions are yet not available for such cases. Thus, in the following, comparisons of the results of the present technique with those obtained analytically are presented for the three major classes discussed above for various functional forms for growth rate, aggregation frequency kernel, nucleation rate and initial condition. We also present one set of results when all the three processes are present to show that the technique can indeed be used for simulating such cases. We then drop one process to enable comparisons with the analytical solutions.

The proposed technique yields numerical solutions in terms of $N_1, N_2, \ldots$ and it appears natural to compare results in terms of them. However, since N_i's depend on the size of the bin which can change from one simulation to other and can become highly irregular due to the particle growth, we will instead compare the two results in terms of average number density defined as

$$\bar{n}_i|_{\text{numerical}} = \frac{N_i}{v_{i+1} - v_i}. \tag{36}$$

The average number density also depends on the size of the bin over which average has been carried out, but this dependence is very weak. The graphs thus display average number densities at the corresponding pivot sizes. To provide a fair comparison, the numerical results have been compared with the analytical average number densities defined as

$$\bar{n}_i|_{\text{analytical}} = \frac{\int_{v_i}^{v_{i+1}} n(v,t)dv}{v_{i+1} - v_i}. \tag{37}$$

and plotted at the same pivot sizes. Numerical solutions have been indicated by symbols and in some figures they have been connected by straight lines to help the reader see the whole size distribution in one glance. The analytical solutions are shown through straight lines joining the data points without explicitly showing the data points through symbols. The discretized initial condition has been indicated by a solid line with symbols on it to show the distribution of pivots at initial time. Since the data points are connected by straight lines, the presence of kinks in the curves is natural.

One last point about the graphs concerns the projection of the symbols or the kinks on the volume axis. As pointed out before, these correspond to the location of the pivots at that time. Movement of pivots, their crowding or dispersion with time therefore directly gives us detailed information about the dynamics of the growth process.

4.1. *Pure Growth.*

4.1.1. $G(v) = \sigma_0 = 1$. We first show our simulation results for the test case that was used in Figs 1(a) and (b) to show the performance of the earlier techniques. The numerical results are obtained by first discretizing the exponential initial distribution using geometrically distributed pivots, shown as symbols on the solid line in Fig. 5. The sets of equations in eq. (32) are solved to obtain new values of x_i's which are then used to estimate numerical average number densities. The analytical average densities were obtained from the following analytical solution:

$$n(v,t) = n_0(v - \sigma_0 t). \tag{38}$$

The figure shows that in comparison with the earlier techniques which did not perform well [as shown in Figs 1(a) and (b)], the present technique yields results that are in excellent agreement with the analytical solutions. In fact, they are hardly distinguishable from the analytical results. Stability and dispersion of the numerical solution which marred the performance of the earlier techniques are completely absent in the present technique.

4.1.2. $G(v) = \sigma_0 v$. Figure 6 shows results for a similar simulations for linear growth function [$\sigma_0 = 1$], and for the same initial condition. The analytical results are obtained using the following analytical solution for the number density.

$$n(v,t) = n_0(ve^{-\sigma_0 t})e^{-\sigma_0 t}. \tag{39}$$

Once again, we see that the numerical results are in excellent agreement with the analytical results.

It is interesting to note that the two forms of the growth rate function simulated in Figs 5 and 6 have resulted in completely different distributions. The constant growth rate function results in very rapid growth rate of small particles while the large particles stay nearly unchanged. This results in narrowing of the size distribution, a feature that is also reflected by the distribution of the pivots in Fig. 5. The linear growth rate function is accompanied by no change in the distribution of the pivots on log scale. In terms of a linear scale, which is what is perceived in practice, the size distribution continues to broaden with time.

4.2. *Simultaneous growth and aggregation*

In this next level of complexity, a total of five analytical solutions are available from Ramabhadran *et al.* (1976). These cases represent various combinations of the constant and linear growth rates, constant and sum aggregation kernels, and exponential and gamma initial distributions. Specific choices of various functions for each case are provided in Table 1.

We have tested our technique for all five cases. The numerical results are obtained for the preservation of

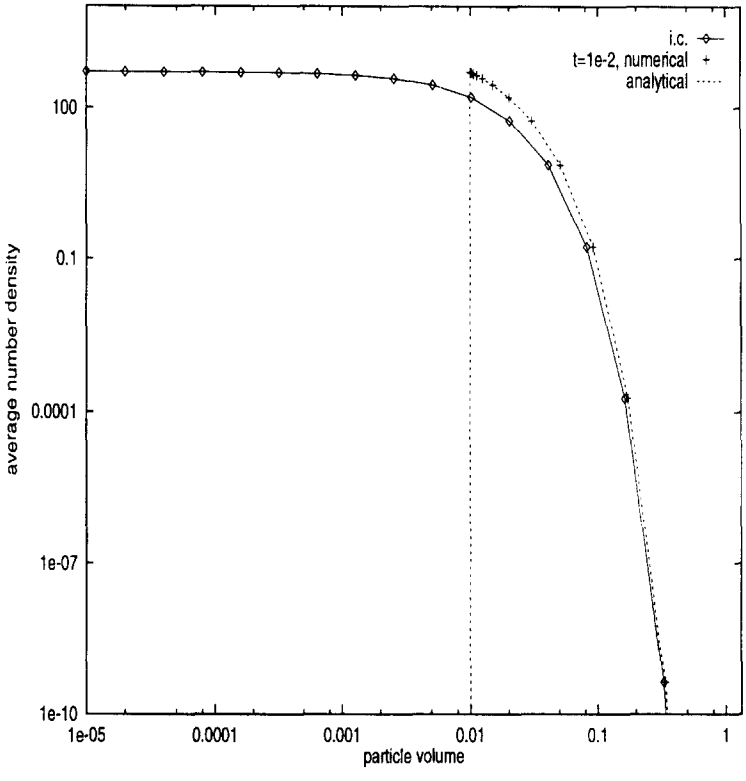

Fig. 5. A comparison of the analytical and numerical results obtained using the proposed technique for the case presented in Figs 1(a) and (b).

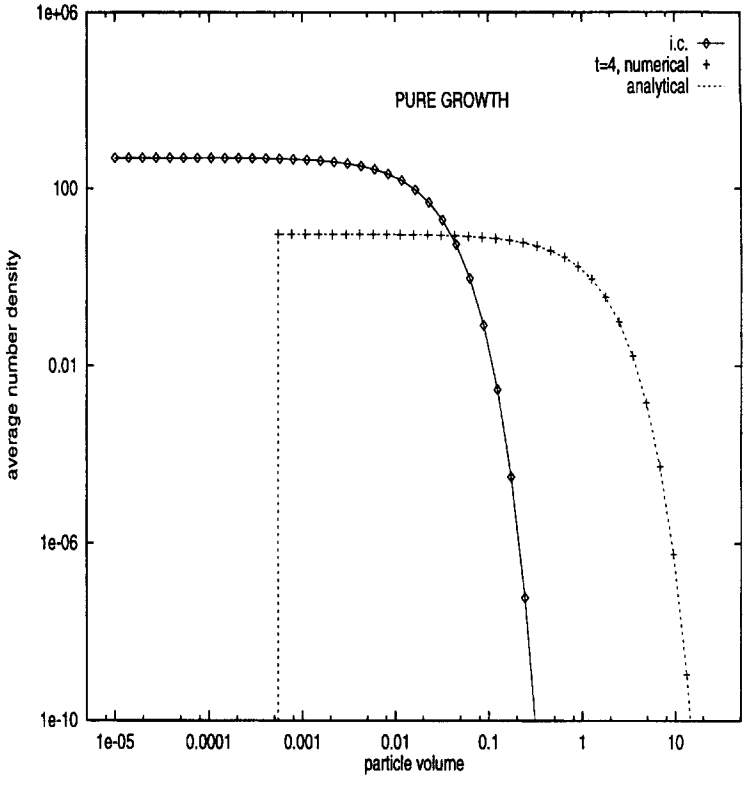

Fig. 6. A comparison of the analytical and numerical results for linear growth [$G(v) = v$] of an exponentially distributed initial population.

Table 1. Various combinations of growth function, aggregation kernel and initial conditions tested for simultaneous growth and aggregation

Case	$G(v)$	$q(v,v')$	$n_0(v)$
1	1	100	$\frac{N_0}{v_{0,i}}\exp(-v/v_{0,i})$
2	1	100	$\frac{N_0}{v_{0,i}}(v/v_{0,i})\exp(-v/v_{0,i})$
3	v	10	$\frac{N_0}{v_{0,i}}\exp(-v/v_{0,i})$
4	v	10	$\frac{N_0}{v_{0,i}}(v/v_{0,i})\exp(-v/v_{0,i})$
5	v	$(v+v')$	$\frac{N_0}{v_{0,i}}\exp(-v/v_{0,i})$

numbers and mass. The procedure adopted for obtaining the numerical solution is the same as that in the previous section. Additionally, the inequalities in eq. (29) are updated periodically (less than 200 times for the largest evolution considered). A *geometric* grid was chosen to cover the size range of interest at the initial time. The smallest size considered in the grid was 1000 times smaller than the parameter $v_{0,i}$ that appears in initial conditions. The latter was fixed at 1×10^{-2} for all simulations presented in this work.

Simulation results for each case have been presented at two times t_1 and t_2. These times and the values of $N(t_1)/N(0)$, $M(t_1)/M(0)$ and $N(t_2)/N(0)$, $M(t_2)/M(0)$ for each case are summarized in Table 2. $N(t)/N(0)$ reflects the extent of aggregation at time t as the growth process conserves numbers. Similarly,

Table 2. Extent of growth ($M(t)/M(0)$) and aggregation ($N(t)/N(0)$) of particles for results shown in Figs 5–10

Case	t_1	$N(t_1)/N(0)$	$M(t_1)/M(0)$	t_2	$N(t_2)/N(0)$	$M(t_2)/M(0)$
1	1.0^{-2}	0.285	1.505	0.1	0.385^{-1}	2.316
2	1.0^{-2}	0.444	1.327	0.1	0.741^{-1}	2.051
3	1	0.384×10^{-1}	2.718	10	0.398×10^{-2}	2.2×10^{4}
4	1	0.739×10^{-1}	2.718	10	0.793×10^{-2}	2.2×10^{4}
5	2	0.756	7.396	3	0.426	20.1

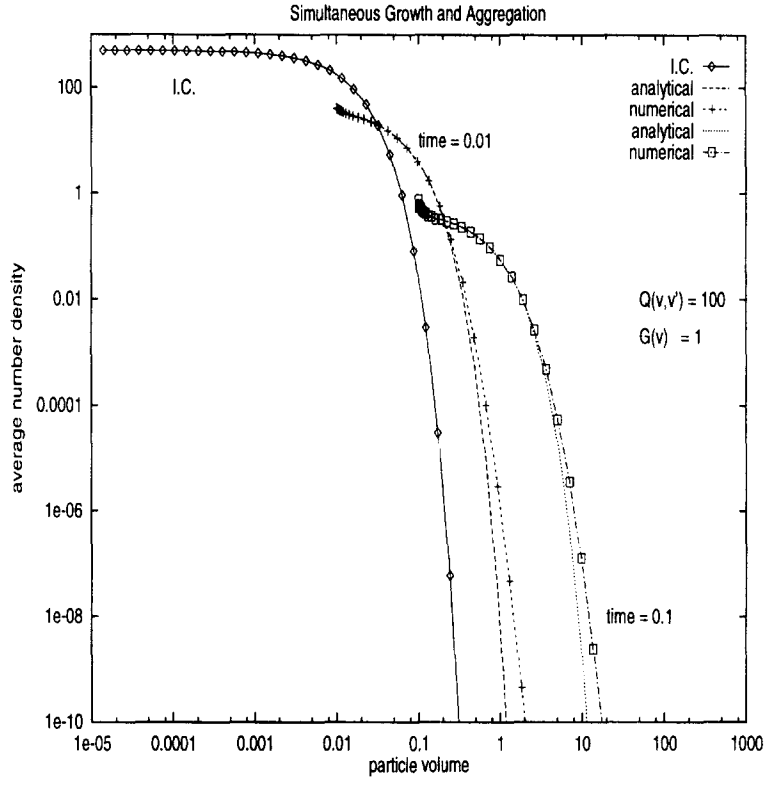

Fig. 7. A comparison of the analytical and the numerical results for simultaneous growth and aggregation, case 1 (Table 1). See Table 2 for the extent of growth and aggregation.

$M(t)/M(0)$ reflects the extent of growth processes at time t as the aggregation process conserves mass.

4.2.1. $G(v) = \sigma_0 q(v, v') = q_0$. Figures 7 and 8 show simulation results for cases 1 and 2 (Table 1), respectively. Both figures indicate that the results are in very good agreement with the analytical results across several orders of magnitude. At very small values of the number density, the results are less than perfect. We would like to point out that for curves such as these, which represent a moving front, the basis of comparison should be the location of the front, and not just a comparison of the values on the y-axis. We have shown in Part I that these deviations occur due to sharply decreasing nature of number density in this size range. If it is desired to have more accuracy in the tail region as well, one can either adopt an overall fine grid or selectively refine the grid in this size range alone to cut down on the number of equations that need to be solved. Both of these approaches have been elucidated in Part I and can be used in the presence of particle growth as well without requiring any modifications.

Large differences that are present on the far left side of the curve for $t = 0.01$ in Fig. 8 and similar but less noticeable differences in all other simulations in Figs 7 and 8 are because the analytical solutions in this range breakdown. Ramabhadran *et al.* (1976) have pointed out that for approximately equal growth and aggregation rates, their analytical solution for $G(v) = \sigma_0$ and $q(v, v') = q_0$ are valid for only large particle sizes. For aggregation-dominated situation, the range of validity is increased, whereas for growth-dominated situation, the solutions break down completely. The simulations

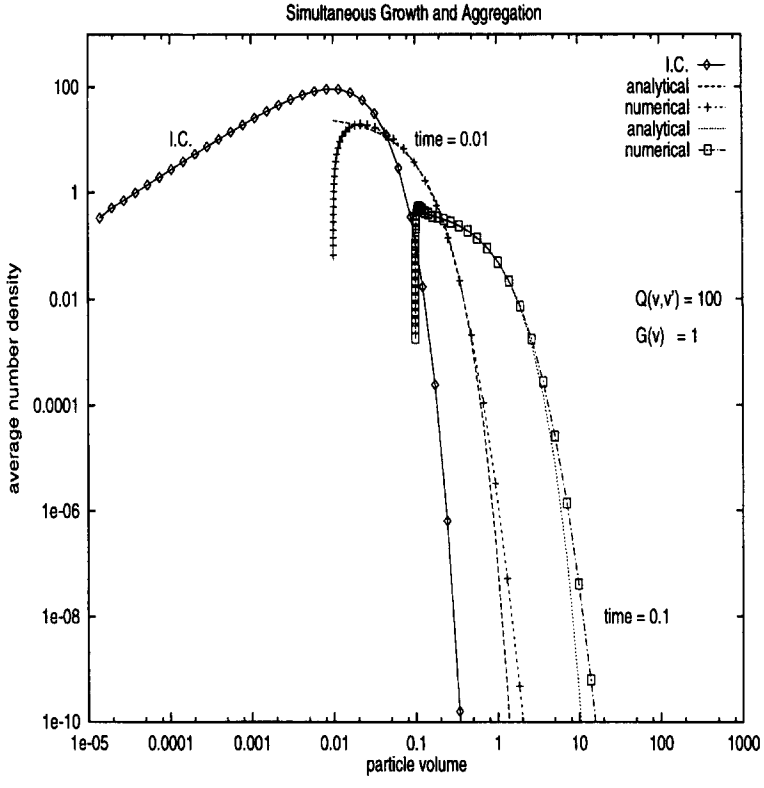

Fig. 8. A comparison of the analytical and the numerical results for simultaneous growth and aggregation, case 2 (Table 1). See Table 2 for the extent of growth and aggregation.

displayed in Figs 7 and 8 correspond to somewhat aggregation-dominated cases to allow analytical solutions to hold in a reasonably wide size range.

As noted before, concentration of pivots in the left region of the curves is reflective of the features of the growth process.

4.2.2. $G(v) = \sigma_0 v, q(v,v') = q_0$. Figures 9 and 10 show evolving size distributions for cases 3 and 4 (Table 1). The numerical results are once again in very good agreement with the analytical results. Location of the front is somewhat overpredicted, but can be improved easily, if needed. Numerical results for $t = 10$ represent very high degree of aggregation and growth (see Table 2), and yet, as the figures show that the numerical results are in excellent agreement across many orders of magnitude for both the initial conditions.

4.2.3. $G(v) = \sigma_0 v, q(v,v') = q_0(v + v')$. Results for case 5, linear growth rate function and the sum kernel for aggregation, are presented in Fig. 11. It shows that even with size-dependent rate functions, the analytical and the numerical results are in excellent agreement.

The above test simulations clearly show that the proposed technique is quite robust and yields very good results for simultaneous growth and aggregation. We therefore believe that in the small particle size range in Figs 7 and 8, where the analytical solutions break down, our numerical solution is correct.

4.3. *Simultaneous nucleation and growth*

4.3.1. $G(v) = \sigma_0$. We start this section with the simulation of the case already shown in Figs 2(a) and (b). Here, $n_0(v) = 0$, $G(v) = 1$ and $S(v) = \dot{N}_{0,n}\delta(v - 1^{-5})$, The simulation results for this case are obtained in exactly the same manner as described in Section 3.3. Starting with one empty bin with $v_1 = x_1 = v_2 = 1 \times 10^{-5}$ and $N_1 = 0$, the following equations are solved for time $\Delta t = 1 \times 10^{-5}$:

$$\frac{dN_1}{dt} = \dot{N}_{0,n} \tag{40a}$$

$$\frac{dv_2}{dt} = G(v_2) \tag{40b}$$

$$\frac{dv_1}{dt} = 0 \tag{40c}$$

$$\frac{dx_1}{dt} = \frac{1}{2}\left(\frac{dv_1}{dt} + \frac{dv_2}{dt}\right). \tag{40d}$$

After time Δt, a new empty bin with the same characteristics as before is introduced and the previous bin is renumbered. We now solve differential equations for N_2, N_1, v_3, x_2, v_2, x_1, v_1 for next Δt units of time and the process continues on. Clearly for $t_{\text{final}} = 0.01$ and $\Delta t = 1^{-5}$, we will end up with solving 3×1000

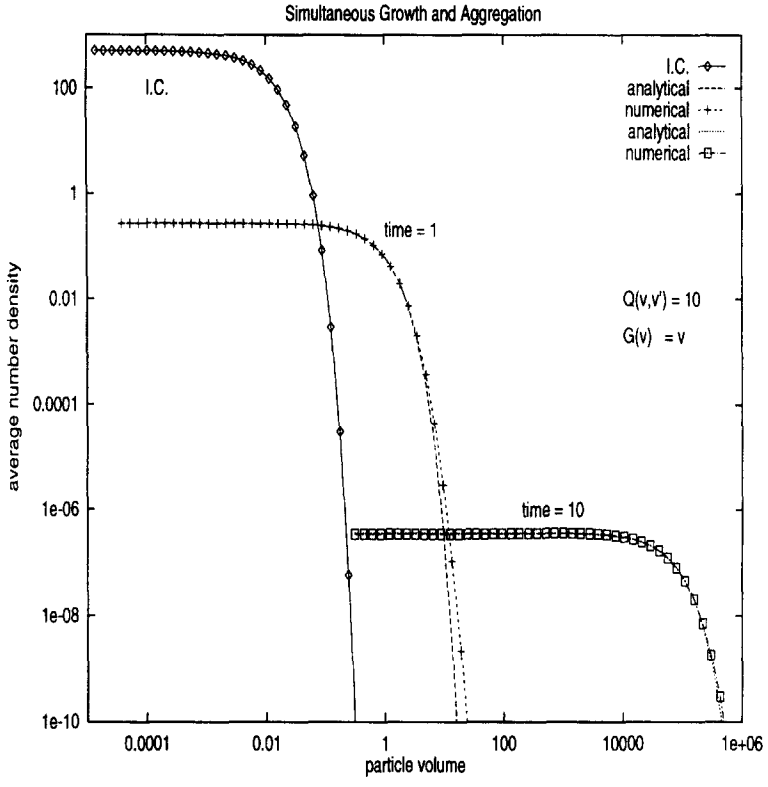

Fig. 9. A comparison of the analytical and the numerical results for simultaneous growth and aggregation, case 3 (Table 1). See Table 2 for the extent of growth and aggregation.

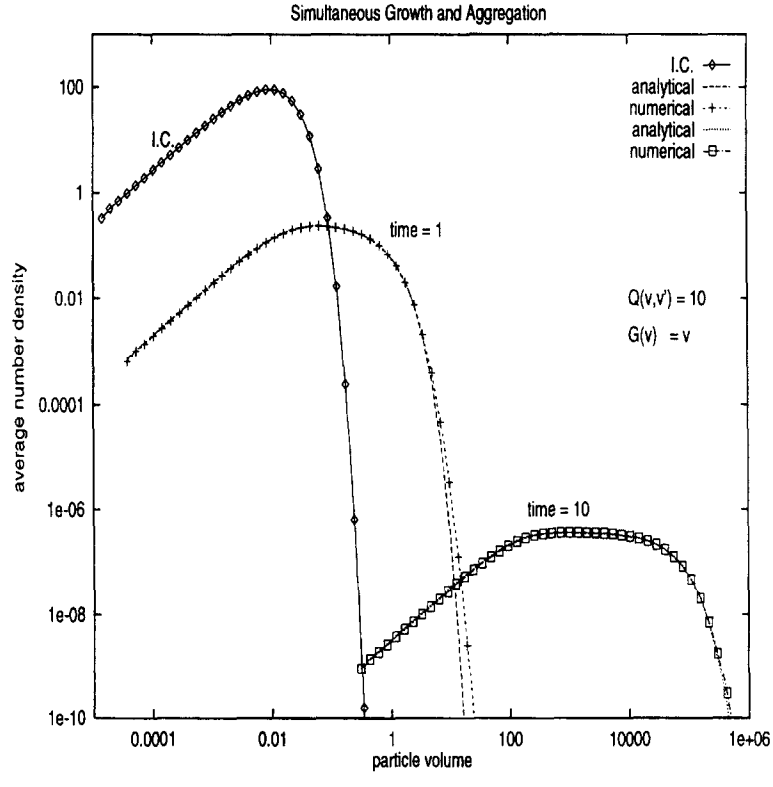

Fig. 10. A comparison of the analytical and the numerical results for simultaneous growth and aggregation, case 4 (Table 1). See Table 2 for the extent of growth and aggregation.

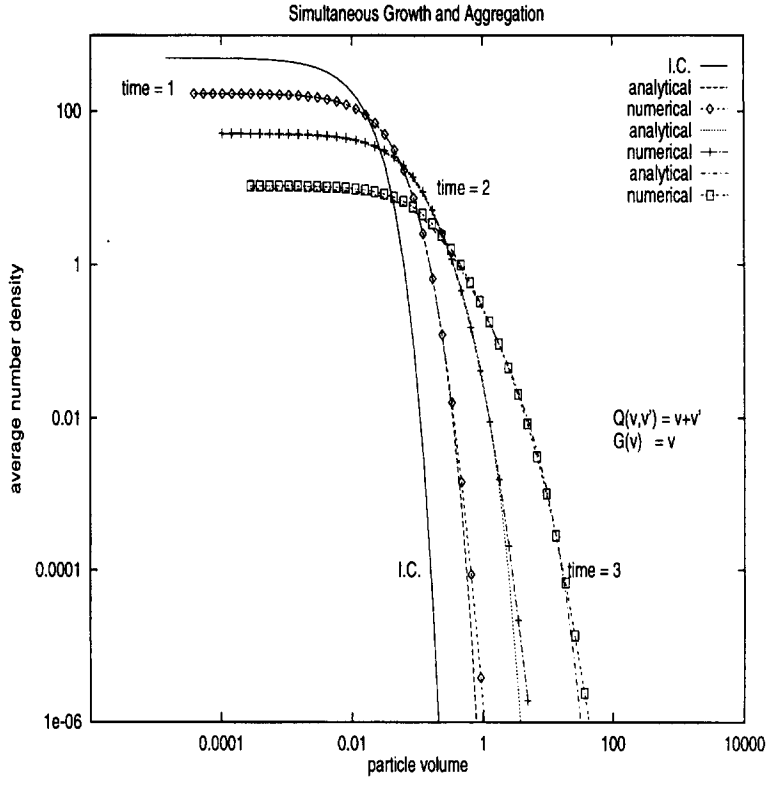

Fig. 11. A comparison of the analytical and the numerical results for simultaneous growth and aggregation, case 5 (Table 1). See Table 2 for the extent of growth and aggregation.

equations towards the end of the simulation. As pointed out in Section 3.3, this is hardly necessary. For any three pivots located such that $x_{i+1}/x_{i-1} < r_{\text{critical}}$, we collapse the ith pivot and assign its population to adjoining pivots, while preserving the properties of interest which in the present case are number and mass. For $r_{\text{critical}} = 1.4$, the maximum number of pivots needed reduces to 28 from 1000. The number of maximum pivots can be further reduced by increasing r_{critical}. If we were to simulate up to $t = 0.1$ with the same Δt, instead of 10,000, only 38 pivots would be needed.

Thus, the proposed method of converting a linear grid generated at the small size end to a coarse, approximately geometric grid as the particles grow bigger, is very efficient at reducing the computational costs. Figure 12 shows that the numerical results obtained using this strategy are in excellent agreement with the analytical results compared with those in Fig. 2. The approximately geometric nature of the grid at particle sizes away from the size of the nuclei is evident from the location of the symbols in the figure.

Of course the implementation of this technique is somewhat involved, but from the view point of computational efficiency and the accuracy of the numerical solution, it is far more effective than the techniques demonstrated in Fig. 2. This is quite clear from this example itself and will become more clear as we demonstrate it for more complex situations.

Figure 13 shows simulation results for the same growth rate but for an exponential distribution of the nuclei sizes (or external feed) $[S(v) = \dot{N}_{0,n}/v_{0,n})\exp(-v/v_{0,n})]$. We further complicate the situation by starting with a pre-existing population, shown as initial condition in the figure. The analytical solution for this case is given as

$$n(v,t) = n_0(v - G(t) + \frac{\dot{N}_{0,n}}{\sigma_0}\left[\exp\left(-\frac{v_{\text{low}}}{v_{0,n}}\right) - \exp\left(-\frac{v}{v_{0,n}}\right)\right], \quad v_{\text{low}} = \max(v_1, v - \sigma_0 t). \tag{41}$$

The simulation strategy is identical to that followed in the previous simulation except that we start with the number of bins needed to discretize the initial distribution plus one empty bin. Bins are added continually at the small size end and collapsed elsewhere to maintain a coarse grid. The figure shows that once again the numerical solutions are in excellent agreement with the analytical solutions.

4.3.2. $G(v) = \sigma_0 v$. The results for this still more complex situation (identical to the previous one except for the size-dependent growth rate) are presented in Fig. 14. The analytical average number densities

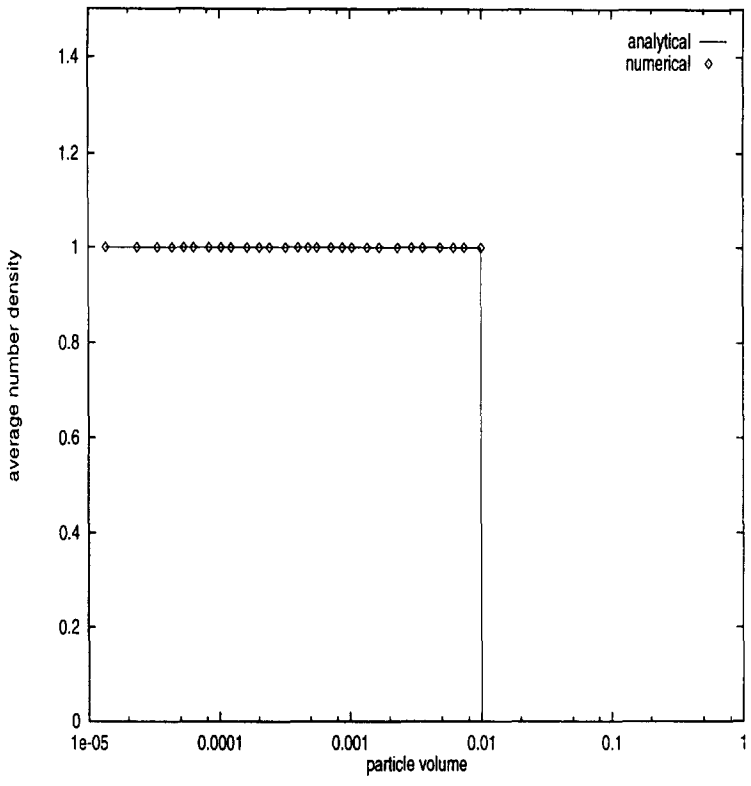

Fig. 12. A comparison of the analytical and the numerical results of the present technique for the case presented in Fig. 2(a) and (b).

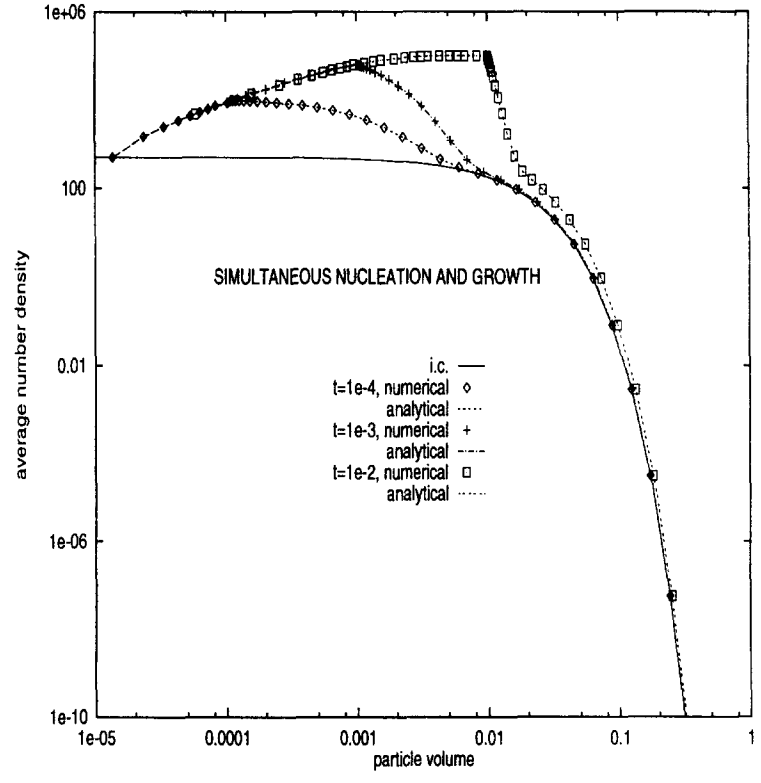

Fig. 13. A comparison of the analytical and the numerical results for simultaneous nucleation [$S(v) = (\dot{N}_{0,n}/v_{0,n}) \exp(-v/v_{0,n})$, $\dot{N}_{0,n} = 10^5$, $v_{0,n} = 10^{-3}$] and constant growth [$G(v) = 1$].

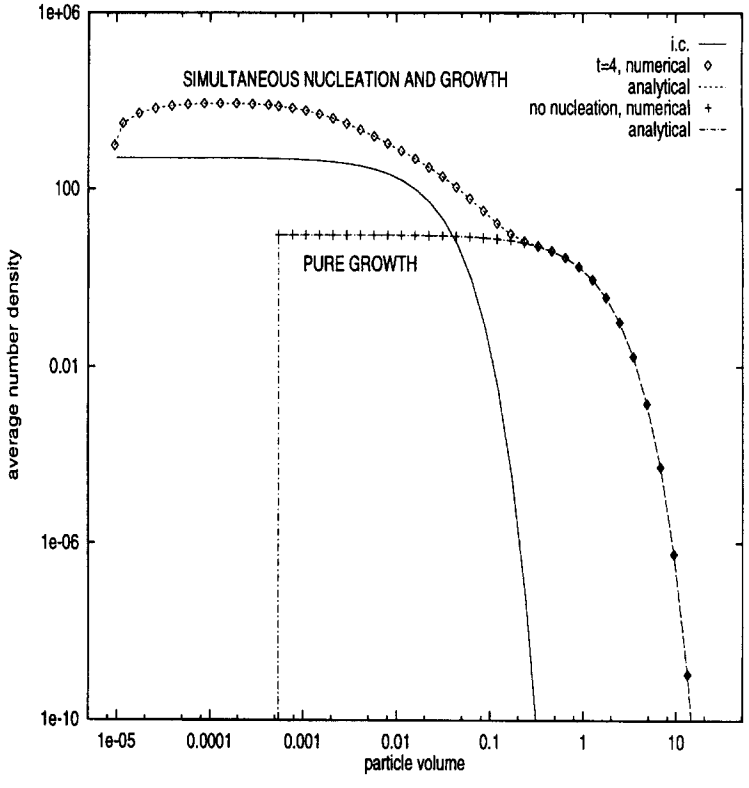

Fig. 14. A comparison of the analytical and the numerical results for simultaneous nucleation [$S(v) = (\dot{N}_{0,n}/v_{0,n})\exp(-v/v_{0,n})$, $N_{0,n} = 10$, $v_{0,n} = 10^{-3}$] and linear growth [$G(v) = 1$].

are obtained from the following analytical solution for number density:

$$n(v,t) = n_0(ve^{-\sigma_0 t})\exp(-\sigma_0 t) + \frac{\dot{N}_{0,n}}{\sigma_0 v}\left[\exp\left(-\frac{v_{\text{low}}}{v_{0,n}}\right) - \exp\left(-\frac{v}{v_{0,n}}\right)\right],$$
$$v_{\text{low}} = \max(v_1, ve^{-\sigma_0 t}) \qquad (42)$$

This situation is more complex in that the new particles are born into old as well as new bins; both types move and also expand with time because the two boundaries of a bin move at different rates for size dependent growth rates. To indicate the extent of nucleation into the old bins, simulation results are also presented for the same case without nucleation. A comparison of the simulation results indicates that when nucleation was allowed, a significant amount of nuclei formed in old bins and were predicted very well. The figure also shows that the technique successfully keeps track of the nucleating and growing particles in the entire size range.

We thus see that the present technique handles simultaneous nucleation and growth very well to produce extremely accurate solutions.

4.4. *Simultaneous nucleation, growth, and aggregation*

The objective of the paper has been to develop a numerical technique that does not suffer from stability and dispersion of the numerical solution, and produces accurate and reliable results for practically relevant case of simultaneous nucleation, growth and aggregation. The usefulness of such a technique will be best determined by testing it for such a case. Unfortunately, analytical solutions for such cases are not easily found. The results presented in this section are therefore only to show that the technique actually applies for the most general case. Limited comparisons with the analytical results are provided after particle aggregation is dropped.

Figure 15 shows simulation results for simultaneous nucleation [$S(v) = (\dot{N}_{0,n}/v_{0,n})\exp(-v/v_{0,n})$], particle growth [$G(v) = \sigma_0$] and aggregation [$q(v,v') = q_0$]. The solution technique is the same as that explained earlier for simultaneous growth and aggregation (Sections 4.1.1 and 4.2) and simultaneous nucleation and growth (Section 4.3.1). The results of the same simulation without the aggregation process are shown in Fig. 16. A comparison of the results in Figs 15 and 16 reveals that the aggregation of particles significantly affects the distribution of particles present initially as well as those born at later times. In fact, the distribution of the nucleated particles, which lie on the left side of discontinuity in the size distributions, is changed completely in the presence of aggregation.

Figure 16 shows that in the absence of aggregation, the agreement between the analytical and the numerical

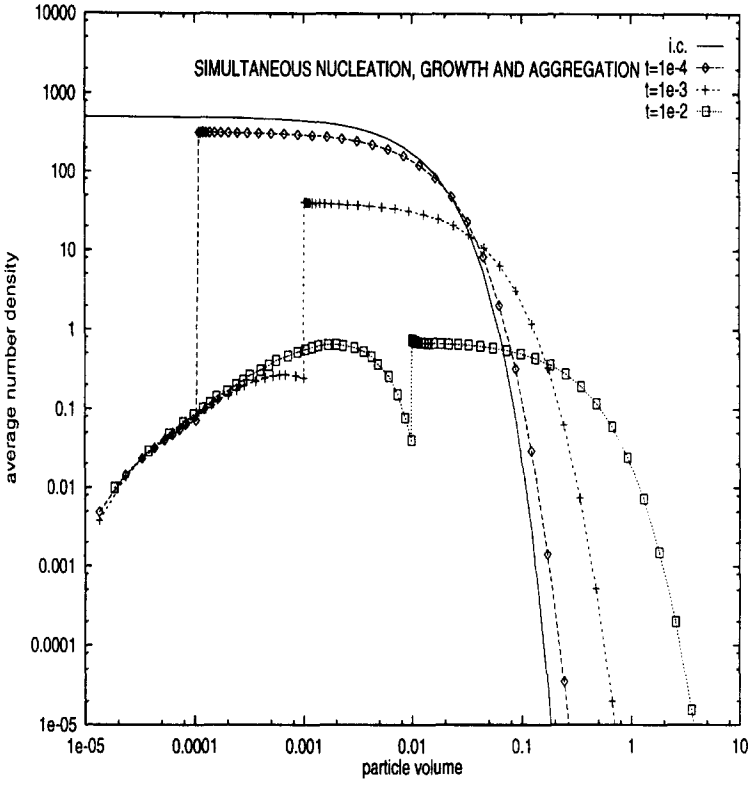

Fig. 15. Simulation results for simultaneous nucleation [$S(v) = \sim (\dot{N}_{0,n}/v_{0,n})\exp(-v/v_{0,n})$, $\dot{N}_{0,n} = 1$, $v_{0,n} = 10^{-3}$], constant growth [$G(v) = 1$] and aggregation [$q(v, v') = 1000$].

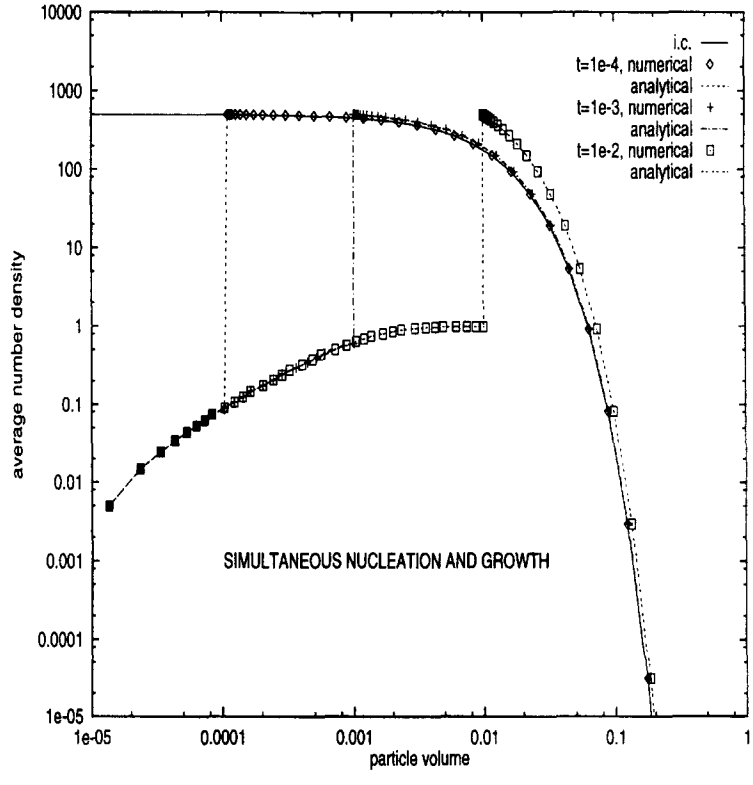

Fig. 16. A comparison of the analytical results with the numerical results for the case presented in Fig. 15 after setting with $q(v, v') = 0$.

results is excellent. When the same simulations are carried out for pure growth and for only growth and aggregation, the agreement between the numerical and the analytical results is very similar to that shown by Figs 5 and 7, respectively. We, therefore, believe that in the light of this evidence, the quality of the numerical results presented in Fig. 15 should be at least as good as that in Fig. 7. for simultaneous growth and aggregation (other combinations result in perfect agreement). The small error that occurs with respect to the location of the front can be improved in ways suggested before in Section 4.2.1.

5. CONCLUSIONS

Discretization techniques for solving PBEs for pure aggregation have been quite successful. However, their finite-difference-type extensions to include growth processes have been rather disappointing as shown earlier in the paper. The reason why it is so is because the presence of growth term which looks much simpler than the formidable aggregation terms introduces a new level of complexity—it introduces hyperbolicity in the governing equations. Discontinuities, no matter how they are introduced, continue to exist at all times. A large number of finite-difference-type formulae (which also formed the basis of the direct extensions proposed by Hounslow *et al.*, Marchal *et al.* and David *et al.*) have already been proposed in the past (Lapidus and Pinder, 1982) and efforts are still continuing in this area. The reason for this continuing pursuit is the unwieldiness of the method of characteristics in situations where the characteristics are not known *a priori.*

Fortunately, for the class of problems of interest in precipitation or crystallization, the characteristics can be determined explicity (for growth rate function being independent of the size distribution) or through an iterative strategy (for growth rate function being influenced by the size distribution through supersaturation). As noted all through in the paper, the solutions obtained after combination method of characteristics with the method of discretization are of excellent quality. Of course, they are slightly more difficult to implement than their finite-difference-type counterpart, but the rewards are far greater and they compensate well for the additional effort.

NOTATION

$G(v)$ growth rate for particles of size v
M total number of equations, or bins considered to represent the size distribution
$M(t)$ total mass present at time t
$n(v,t)$ number density of particles of size v
$n_0(v)$ initial number density (i.c.)
$N(t)$ total number of particles at time t
N_i total population of ith size range, time dependent
$\dot{N}_{0,n}$ rate of nucleation of particles of all sizes
$q(v,v')$ aggregation frequency between particles of size v and v'
q_0 constant aggregation rate, $(v,v') = q_0$
r defined as v_{i+1}/v_i
$S(v)$ rate of nucleation of particles of size v
v_i size of the smallest particle in ith bin, time-dependent
v_{i+1} size of the largest particle in ith bin, time-dependent
Δv_i width of the ith size range, $v_{i+1} - v_i$
$v_{0,i}$ a parameter in gamma or exponential initial condition
$v_{0,n}$ a parameter in exponentially distributed nucleation rate
x_i representative volume (pivot) for ith size range, time dependent

Greek letters

$\alpha_{i,j,k}, \beta_{i,j}$ coefficients used to represent discretized version of coagulation terms. See Kumar and Ramkrishna (1996) for details.
$\delta(v), \delta_{i,j}$ Dirac-delta function
σ_0 a parameter in growth rate function, $G(v) = \sigma_0$ or $\sigma_0 v$

REFERENCES

Baterham, R. J., Hall, J. S. and Barton, G. (1981) Pelletizing kinetics and simulation of full scale balling circuits. *Proceedings of the 3rd International Symposium on Agglomeration*, Nurnberg, W. Germany, p. A136.

David, R., Villermaux, J., Marchal, P. and Klein, J. P. (1991) Crystallization and precipitation engineering—IV. Kinetic model fo adipic acid crystallization. *Chem. Engng Sci.* **46**, 1129–1136.

Gelbard, F. (1990) Modeling multicomponent aerosol particle growth by vapor condensation. *J. Aerosol Sci. Technol.* **12**, 399–412.

Gelbard, F. and Seinfeld, J. H. (1978) Numerical simulation the dynamic equation for particulate systems, *J. Comput. Phys.* **28**, 357–375.

Hounslow, M. J., Ryall, R. L. and Marshall, V. R. (1988) A discretized population balance for nucleation, growth and aggregation. *A.I.Ch.E. J* **34**, (1990) 1821–1832.

Kim, Y. P. and Seinfeld, J. H. (1990) Simulation of multicomponent aerosol condensation by moving ectional method. *J. Colloids Interface Sci.* **135**, 185–199.

Kostoglou, M. and Karabelas, A. J. (1994) Evaluation of zero order methods for simulating particle coagulation. *J. Colloidal Interface Sci.* **613**, 420–431.

Lapidus, L. and Pinder, G. F. (1982) *Numerical Solution of Partial Differential Equations in Science and Engineering.* Wiley, New York, U.S.A.

Marchal, P., David, R., Klein, J. P. and Villermaux, J. (1990) Crystallization and precipitation engineering—1. An efficient method for solving population balances in crystallization with agglomeration. *Chem. Engng Sci.* **43**, 59–67.

Middleton, P. and Brock, J. (1976) Simulation of aerosol kinetics. *J. Colloidal Interface Sci.* **54**, 249–264.

Muhr, H., David, R., Villermaux, J. and Jezequel, P. H. (1995) Crystallization and precipitation engineering—V. Simulation of the precipitation of silver bromide octahedral crystals in a double-jet semi-batch reactor. *Chem. Engng Sci.* **50**, 345–355.

Muhr, H., David, R., Villermaux, J. and Jezequel, P. H. (1996) Crystallization and precipitation engineering—VI. Solving population balance in the case of the precipitation of silver bromide crystals with high primary nucleation rates by using the first order upwind differentiation. *Chem. Engng Sci.* **51**, 309–319.

Ramabhadran T. E., Peterson, T. W. and Seinfeld, J. H. (1976) Dynamics of aerosol coagulation and condensation. *A.I.Ch.E. J.* **22**, 840–851.

Ramkrishna, D. (1985) The status of population balances. *Rev. Chem. Engng* **3**, 49–95.

Kumar, S. and Ramkrishna, D. (1996) On the solution of population balance equations by discretization—I. A. fixed pivot technique. *Chem. Engng Sci.* **51**, 1311–1332.

Schiesser, W. E. (1991) *The Numerical Method of Lines, Integration of Partial Differential Equations.* Academic Press, Inc., Sand Diego, U.S.A.